British Journal of Pharmacology

British Journal of Pharmacology (2016) **173** 3145–3158 3145

RESEARCH PAPER

Mitochondrial uncoupler carbonyl cyanide m-chlorophenylhydrazone induces vasorelaxation without involving K_{ATP} channel activation in smooth muscle cells of arteries

Correspondence Professor De-Li Dong, Department of Pharmacology, Harbin Medical University, Baojian Road 157, Harbin 150086, Heilongjiang Province, China. E-mail: dongdeli@ems.hrbmu.edu.cn

Received 16 April 2016; **Revised** 16 August 2016; **Accepted** 16 August 2016

Yan-Qiu Zhang, Xin Shen, Xiao-Lin Xiao, Ming-Yu Liu, Shan-Liang Li, Jie Yan, Jing Jin, Jin-Lai Gao, Chang-Lin Zhen, Nan Hu, Xin-Zi Zhang, Yu Tai, Liang-Shuan Zhang, Yun-Long Bai and De-Li Dong

Department of Pharmacology (the State-Province Key Laboratories of Biomedicine-Pharmaceutics of China, Key Laboratory of Cardiovascular Research, Ministry of Education), College of Pharmacy; Translational Medicine Research and Cooperation Center of Northern China, Heilongjiang Academy of Medical Sciences, Harbin Medical University, Harbin, PR China

BACKGROUND AND PURPOSE

The effects and mechanisms of chemical mitochondrial uncouplers on vascular function have never been identified. Here, we characterized the effects of the typical mitochondrial uncoupler carbonyl cyanide m-chlorophenylhydrazone (CCCP) on vascular function in rat mesenteric arteries and aorta and elucidated the potential mechanisms.

EXPERIMENTAL APPROACH

Isometric tension of mesenteric artery and thoracic aorta was recorded by using a multiwire myograph system. Protein levels were measured by western blot analyses. Cytosolic $[Ca^{2+}]_i$, mitochondrial ROS (mitoROS) and mitochondrial membrane potential of smooth muscle cells (A10) were measured by laser scanning confocal microscopy.

KEY RESULTS

Acute treatment with CCCP relaxed phenylephrine (PE)- and high K^+ (KPSS)-induced constriction of rat mesenteric arteries with intact and denuded endothelium. Pretreatment with CCCP prevented PE- and KPSS-induced constriction of rat mesenteric arteries with intact and denuded endothelium. Similarly, CCCP prevented PE- and KPSS-induced constriction of rat thoracic aorta. CCCP increased the cellular ADP/ATP ratio in vascular smooth muscle cells (A10) and activated AMPK in A10 cells and rat thoracic aorta tissues. CCCP-induced aorta relaxation was attenuated in AMPK α1 knockout (−/−) mice. SERCA inhibitors thapsigargin and cyclopiazonic acid (CPA) but not the K_{ATP} channel blocker glibenclamide partially inhibited CCCP-induced vasorelaxation in endothelium-denuded rat mesenteric arteries. CCCP increased cytosolic $[Ca^{2+}]_i$, mitoROS production and depolarized mitochondrial membrane potential in A10 cells. FCCP, the analogue of CCCP, had similar vasoactivity as CCCP in rat mesenteric arteries.

CONCLUSIONS AND IMPLICATIONS

CCCP induces vasorelaxation by a mechanism that does not involve K_{ATP} channel activation in smooth muscle cells of arteries.

Abbreviations

CCCP, carbonyl cyanide m-chlorophenylhydrazone; CPA, cyclopiazonic acid; FCCP, carbonylcyanidep-trifluoro-methoxyphenylhydrazone; 5-HD, 5-hydroxydecanoic acid; mitoROS, mitochondrial ROS; PE, phenylephrine; TMRM, tetramethylrhodamine methyl ester; UCPs, mitochondrial uncoupling proteins; SERCA, sarco-endoplasmic reticulum Ca^{2+} ATPase

DOI:10.1111/bph.13578

Tables of Links

TARGETS	
Voltage-gated ion channels[a]	**Transporters**[c]
BK_{Ca} (K_{Ca} 1.1) channel	SERCA
K_{ATP} (K_{ir}3.4) channel	
Enzymes[b]	
AMPK	
eNOS	

LIGANDS	
ACh	Paxilline
CPA (cyclopiazonic acid)	Phenylephrine
Diazoxide	Thapsigargin
Glibenclamide	

These Tables list key protein targets and ligands in this article which are hyperlinked to corresponding entries in http://www.guidetopharmacology.org, the common portal for data from the IUPHAR/BPS Guide to PHARMACOLOGY (Southan *et al.*, 2016) and are permanently archived in the Concise Guide to PHARMACOLOGY 2015/16 ([a,b,c]Alexander *et al.*, 2015a,b,c).

Introduction

In normally functioning mitochondria, the transport of electrons to oxygen is coupled to the formation of ATP via a proton electrochemical gradient. Mitochondrial uncoupling proteins (UCPs) or chemical mitochondrial uncouplers can induce proton leak from the intermembrane space into the mitochondrial matrix, preventing the development of a proton electrochemical gradient, thus reducing ATP production. This process is named as mitochondrial uncoupling. Recently, mild mitochondrial uncoupling has been proposed as a protective therapeutic strategy for many disorders, for instance, diabetes, obesity and hyperlipidaemia (Diano and Horvath, 2012; Busiello *et al.*, 2015).

Among the UCPs, UCP2 is considered to be important in cardiovascular pathophysiology; thus, the role of mitochondrial uncoupling in regulating cardiovascular function has been intensively studied by using UCP2 transgenic and knockout mice models. UCP2 preserves the endothelial function of obese diabetic mice by increasing nitric oxide bioavailability secondary to the inhibition of ROS production in endothelium (Tian *et al.*, 2012) and prevents salt-sensitive hypertension through the same mechanisms in mice (Ma *et al.*, 2010). Adenovirus-mediated UCP2 overexpression inhibits atherosclerotic processes of cultured human vascular smooth muscle cells in response to high glucose and angiotensin II (Ang II; Park *et al.*, 2005) and inhibits the apoptosis of human aortic endothelial cells by suppressing ROS production (Lee *et al.*, 2005). These studies by using UCP2 transgenic or knockout models demonstrate the relatively chronic effects of mitochondrial uncoupling on vascular function, but the acute effect of mitochondrial uncoupling on vascular function is still unclear. In particular, the effects and mechanisms of mitochondrial uncoupling on vascular function have never been systematically studied using small chemical uncouplers, which would have more potential for clinic use than transgenic or knockout techniques.

Carbonyl cyanide m-chlorophenylhydrazone (CCCP) is a typical mitochondrial uncoupler, which is widely used in studies on mitochondrial uncoupling. Earlier work in the 1980s showed that CCCP prevented noradrenaline-induced contractions in rabbit mesenteric arteries (Haeusler *et al.*, 1981). A recent study used CCCP to investigate the physiological functions of SUR2-containing K_{ATP} channels in mediating vasodilatation, based on the speculation that CCCP would activate K_{ATP} channels in mouse cerebral arteries (Adebiyi *et al.*, 2011). In the present study, we characterized the effects of the mitochondrial uncoupler CCCP on vascular function in rat mesenteric arteries and aorta and elucidated the potential mechanisms. We found that CCCP induces vasorelaxation in smooth muscle cells of arteries by a mechanism that does not involve K_{ATP} channel activation.

Methods

Animals

Adult Sprague–Dawley rats (male, body weight 320–350 g, 8–10 weeks) were purchased from Charles River (Charles River Laboratory Animal, Beijing, China). The AMPK α1 knockout (−/−) mice (background C57BL/6 strain, 8 weeks) were a kind gift from Prof. Hong-Liang Li (Collaborative Innovation Center of Model Animal Wuhan University). A total of eighty rats, six wide-type mice and two AMPK α1 knockout (−/−) mice were used in the study. The rats were maintained in groups of six animals per cage (1300 cm^2) and the mice in groups of three to five animals per cage (530 cm^2) on a 14 h light and 10 h dark circadian rhythm with water and food available *ad libitum*. The AMPK α1 knockout (−/−) mice were anaesthetized with sodium pentobarbitone (50 $mg \cdot kg^{-1}$, i.p.) before being killed. Genotyping of AMPK α1 knockout (−/−) mice by PCR was performed using the following three primers: primer 1:5′-GCTTAGGTCCTCATCACTG-3′, 5′-CTTGATCATCAACTCCCAGG-3′, 5′-CGCCTTCTTGACG-AGTTC-3′. Their wild-type littermates were used as controls. All the experimental procedures were approved by the Institutional Animal Care and Use Committee of Harbin Medical University, China. Animal studies are reported in compliance with the ARRIVE guidelines (Kilkenny *et al.*, 2010; McGrath and Lilley, 2015).

Rat mesenteric artery and thoracic aorta preparation

Adult male Sprague–Dawley rats (300–400 g) were killed after being anaesthetized with sodium pentobarbitone

(40 mg·kg^{-1}, i.p.). The entire mesentery and thoracic aorta was removed quickly, then transferred into cold (4°C) modified physiological salt solution (PSS) with the following composition (mM): NaCl, 130; KCl, 4.7; $MgSO_4 \cdot 7H_2O$, 1.17; KH_2PO_4, 1.18; $NaHCO_3$, 14.9; $CaCl_2$, 1.6; D-glucose, 5.5 (PH 7.35–7.45). Fat tissue was removed from the mesenteric artery and thoracic aorta and the mesenteric arteries and thoracic aorta were dissected into 2-mm and 3–4-mm rings respectively.

Isometric tension recording of mesenteric artery and thoracic aorta

The experiments were carried out according to our previous work (Chen *et al.*, 2010; Wang *et al.*, 2013). The mesenteric artery and thoracic aorta rings were randomized for different treatments. Mesenteric arterial ring was mounted between two wires and fixed in the bath filled with 5 mL PSS and were continuously bubbled with gas (95% O_2 + 5% CO_2). Thoracic aortic rings were mounted on a triangle-shaped hook and then suspended in the bath filled with 10 mL PSS that was continuously bubbled with gas (95% O_2 + 5% CO_2). The isometric contractions of mesenteric arterial rings were measured by using a multiwire myograph system (model 620 DMT, Danish Myo Technology, Denmark), and the isometric contractions of thoracic aortic rings were measured by using a multichannel myograph system (BL-420S, Chengdu Taimeng Software CO.LTD., China). The arterial rings were equilibrated for 60 min, and then a wake-up protocol was performed to reactivate the mechanical, functional and signalling properties of the vessels by using high K^+ PSS (KPSS) and PE as stimuli. The KPSS (60-mM K^+) solution for inducing vasoconstriction was composed of (mM) NaCl, 74.7; KCl, 60; $MgSO_4 \cdot 7H_2O$, 1.17; KH_2PO_4, 1.18; $NaHCO_3$, 14.9; $CaCl_2$, 1.6; D-glucose, 5.5; EDTA, 0.026. In order to avoid the error induced by natural rundown of the artery tension, we calculated the relaxation ratio of CCCP by subtracting the relaxation ratio of a corresponding control (DMSO). Because a natural relaxation of artery tension occurred in the control group, the relaxation response to CCCP will appear to be smaller compared with the original recording traces as the relaxation is expressed as a ratio relative to its corresponding control (DMSO).

Measurement of mitochondrial ROS

Cultured arterial smooth muscle cells (A10) were loaded with MitoSOX (2 μM) for 20 min and hoechst (1 μg·m^{-1}) for 15 min at 37°C, and then the fluorescence was measured by using confocal microscopy. Confocal microscope images were collected by using a Zeiss LSM 700 with the Zeiss LSM software. Images of MitoSOX fluorescence were obtained using a 40 × oil objective with an excitation at 555 nM and an emission of 585 nM. Images of hoechst staining were obtained by using excitation at 405 nM and an emission of 435 nM. The relative intensity of the fluorescence represents the level of mitochondria ROS (mitoROS).

Measurement of cytosolic $[Ca^{2+}]_i$ of smooth muscle cells

Cultured arterial smooth muscle cells (A10) were loaded with 5 μM fluo-3 AM for 15 min(37°C) and rinsed four times with warm PBS (37°C). The fluorescence was measured by using confocal microscopy (Zeiss LSM 700; Zeiss; Oberkochen, Germany). The excitation and emission wavelength for signal detection was 488 and 518 nM respectively. The relative intensity of the fluorescence indicates the levels of cytosolic $[Ca^{2+}]_i$.

Measurement of mitochondrial membrane potential by TMRM

Cultured arterial smooth muscle cells (A10) were loaded with TMRM (50 nM) for 45 min and Hoechst (1 μg·mL^{-1}) for 15 min at 37°C, and were then rinsed four times with warm PBS (37°C), then the fluorescence was measured by using confocal microscopy. Confocal microscope images were obtained by using a Zeiss LSM 700 with the Zeiss LSM software. Images of TMRM fluorescence were obtained using a 20 × objective lens with an excitation at 535 nM and an emission of 600 nM. Images of Hoechst staining were obtained by using excitation at 405 nM and an emission of 435 nM. The relative intensity of the fluorescence indicates the mitochondrial membrane potential.

Western blot experiments

These experiments were carried out as described previously (Sun *et al.*, 2013; Xie *et al.*, 2015). Briefly, proteins were extracted with lysis buffer containing 1% protease inhibitor and 10% phosphatase inhibitor solution. Concentrations of proteins were measured by use of a BCA Protein Assay Kit. Proteins were separated by 8% SDS-PAGE and blotted onto nitrocellulose membranes. Membranes were incubated with antibodies at 4°C over night. Membranes were incubated with fluorescence-conjugated secondary antibodies (1:10 000 dilution, LI-COR) for 1 h. Western blot bands were quantified by using an Odyssey infrared imaging system (LI-COR, Lincoln, Nebraska, USA) and Odyssey v3.0 software.

Measurement of ATP concentration

The amount of ATP was measured by the luciferin–luciferase method following the protocol of an ATP detection kit (Beyotime, Shanghai, China). The cells were collected on ice and immediately lysed with 30 μL lysis buffer from the ATP detection kit. After being centrifuged at 12 000 *g* for 5 min at 4°C, the supernatant was transferred to a new 1.5 mL tube for the ATP test. The luminescence from a 20 μL sample was assayed in a luminometer (GloMax®20/20 Promega, Madison, WI, USA) together with 100 μL ATP detection buffer in the ATP detection kit. The standard curve of ATP concentration was prepared from known amounts (0.1–10 μM). The ATP concentrations in the samples were normalized to the amount of protein (μmol·mg^{-1} protein), measured by use of a BCA assay kit (P0010 Beyotime, China).

Measurement of ADP/ATP ratio

The ADP/ATP ratio was measured by use of an ADP/ATP-Lite Assay Kit (Vigorous Bio, Beijing, China). The cells were collected on ice and immediately lysed with 30 μL lysis buffer from the kit. After vortexed fully for 30 s and centrifuged for 30 s, the supernatant was transferred to another 1.5 mL tube for the ratio test. The luminescence of the ATP content (RLU_A) was assayed in a luminometer (GloMax®20/20 Promega, USA) with 5 μL sample and 50 μL ATP detection buffer in a new

1.5 mL tube. After this sample had been kept in the dark for 10 min, the luminescence of the residual ATP content (RLU_B) was obtained. Then 5 μL of ATP converting enzyme from the kit was added to the tube. After 10 min incubation, the luminescence was again read to obtain RLU_C. The ADP/ATP ratio was calculated using the formula: ADP/ATP ratio = $(RLU_C - RLU_B)/ RLU_A$.

Statistical analysis

Data are presented as mean ± SEM. Significance was determined by using Student's *t*-test for comparison of two groups, or one-way ANOVA for two or more groups followed by Tukey's test. All statistical tests were performed using SigmaPlot (12.5 verison). $P < 0.05$ was considered significant. The data and statistical analysis comply with the recommendations on experimental design and analysis in pharmacology (Curtis *et al.*, 2015).

Materials

Arterial smooth muscle cells (A10) were purchased from ATCC (Manassas, Virginia, USA). Phenylephrine (PE) was purchased from Shanghai Harvest Pharmaceutical Co.LTD., China. CCCP, carbonylcyanidep-trifluoro-methoxyphenylhydrazone (FCCP), 5-hydroxydecanoic acid (5-HD), cyclopiazonic acid (CPA), thapsigargin, ACh and mitoTEMPO were purchased from Sigma Aldrich Chemistry (Saint Louis, MO, USA). MitoSOX, fluo-3/AM, tetramethylrhodamine methyl ester (TMRM) and hoechst were purchased from Life Technology (Invitrogen, OR, USA). Glibenclamide and endothelial NOS (eNOS) antibody were purchased from Santa Cruz Biotechnology (Dallas, Texas, USA). Paxilline (Pax) was purchased from Cayman Chemical Company (Ann Arbor, Michigan, USA). AMPK, p-AMPK (Thr^{172}), p-eNOS (Ser^{1177}) antibodies were purchased from Cell Signaling Technology (Danvers, MA, USA). PE and ACh were dissolved in distilled water, and other reagents were dissolved in DMSO (Tianjin Fuyu Fine Chemical Co., Ltd, Tianjin, China).

Results

CCCP relaxes PE- and high KPSS-induced constriction of rat mesenteric arteries

Firstly, we examined the effects of CCCP on PE- and KPSS-induced constriction of rat mesenteric arteries with intact endothelium. The intact-endothelium of mesenteric arteries was confirmed by the presence of an ACh-induced relaxation response (Figure 1A). As shown in Figure 1B–E, CCCP induced concentration-dependent relaxation in endothelium-intact rat mesenteric arteries precontracted with PE and KPSS. The original recordings are shown in Figure 1B and D, and the summarized data are shown in Figure 1C and E. In rat mesenteric arteries with denuded endothelium, CCCP also showed relaxant effects on the pre-contraction induced by PE and KPSS (Figure S1). These results indicate that the vasorelaxant activity of CCCP is endothelium-independent.

CCCP pretreatment prevents PE- and high KPSS-induced constriction of rat mesenteric arteries

Next, we investigated whether CCCP pretreatment could prevent PE- and KPSS-induced vasoconstriction. As shown in Figure 2A and B, CCCP pretreatment for 20 min significantly prevented PE- and high K^+-induced constriction of rat mesenteric arteries with intact endothelium, and this inhibition was removed after washout of CCCP. In rat mesenteric arteries with denuded endothelium, CCCP pretreatment showed a similar preventive action (Figure S2).

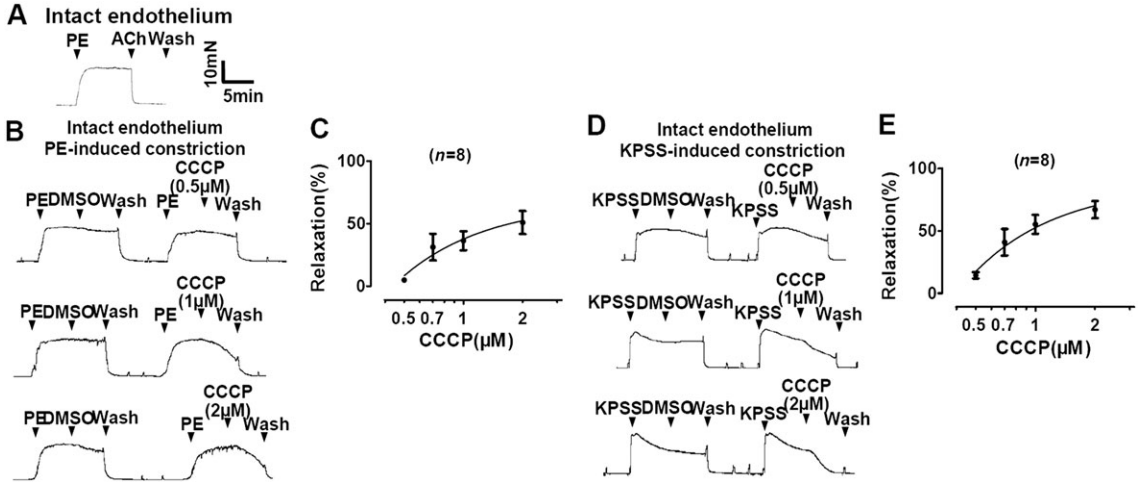

Figure 1

CCCP relaxes PE- and high KPSS-induced constriction of rat mesenteric arteries with intact endothelium. (A) Original trace demonstrating endothelium-intact rat mesenteric artery. The artery was precontracted with PE (5 μM) and relaxed by ACh (1 μM). (B,C) Original traces showing that CCCP induced dose-dependent relaxation in endothelium-intact rat mesenteric arteries precontracted with PE (5 μM) and the summarized data. The relaxation ratio of CCCP was calculated by subtracting the relaxation ratio of corresponding control (DMSO) to avoid the error induced by natural rundown of the artery tension. (D,E) Original traces showing that CCCP induced dose-dependent relaxation in endothelium-intact rat mesenteric arteries precontracted with KPSS and the summarized data. The relaxation ratio of CCCP was calculated by subtracting the relaxation ratio of corresponding control (DMSO) to avoid the error induced by natural rundown of the artery tension.

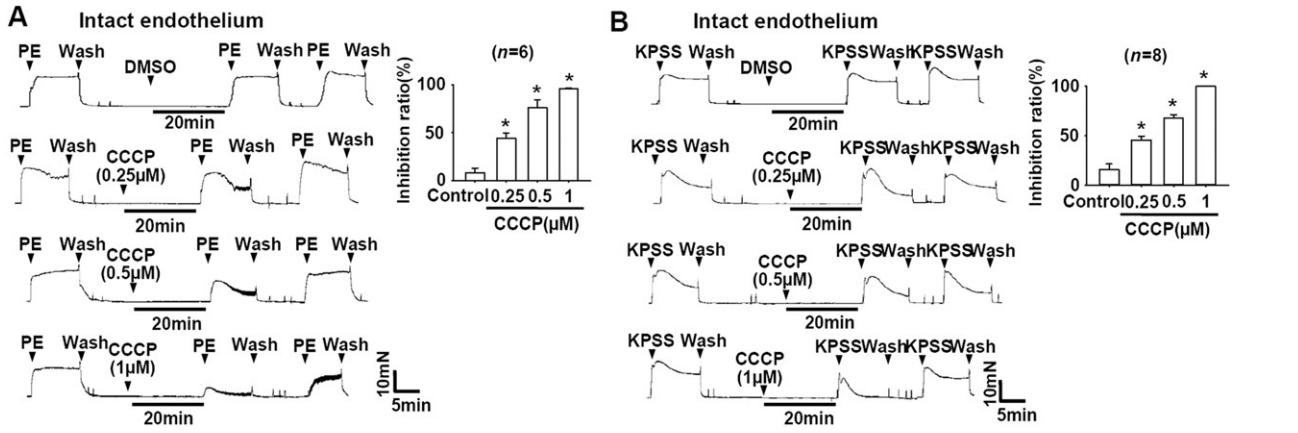

Figure 2

CCCP pretreatment prevents PE- and KPSS-induced constriction of rat mesenteric arteries with intact endothelium. The inhibitory effect of CCCP was removed after washout of CCCP. $^{**}P < 0.01$ versus DMSO (control).

CCCP inhibits PE- and high KPSS-induced constriction of rat thoracic aorta

In order to test whether CCCP had similar inhibitory effects on the vasoconstriction in large conduit arteries, we examined the effects of CCCP on the rat thoracic aorta. As shown in Figure 3A–C, CCCP relaxed PE- and KPSS-induced vasoconstriction of the rat thoracic aorta with intact endothelium. In rat thoracic aorta with denuded endothelium, CCCP showed similar relaxation effects on PE- and KPSS-induced vasoconstriction (Figure S3). Although CCCP relaxed the vasoconstriction in both rat mesenteric arteries and thoracic aorta, of note, the mesenteric arteries were more sensitive than the aorta to the effects of CCCP.

Additionally, we further examined the effects of CCCP on eNOS activity in HUVECs. CCCP (1 and 10 μM) did not affect the expressions of eNOS and p-eNOS protein in HUVECs after a 5 and 15 min treatment (Figure S4), confirming the endothelium-independent effects of CCCP.

CCCP activates AMPK in vascular smooth muscle cells and rat thoracic aorta tissues

Mitochondrial uncouplers can reduce cellular ATP levels and activate AMPK (Soltoff, 2004; Eskiocak *et al.*, 2014; Figarola *et al.*, 2015). We examined the effects of CCCP on cellular ATP levels and the ADP/ATP ratio in vascular smooth muscle cells (A10). CCCP (2 μM) did not affect the cellular ATP level after 5 min treatment, but reduced the cellular ATP level after 20 min treatment (Figure 4A). However, an increased ADP/ATP ratio was detected after CCCP treatment for 5 min even when the ATP level was not changed (Figure 4B). These phenomena were speculated to be due to CCCP initially inducing a compensatory increase in ATP production and an increase in ADP hydrolyzed from ATP. However, the production and consumption of ATP were balanced at 5 min, so the ATP level was not significantly changed. With the time lapse (20 min), the inhibition of ATP synthase by CCCP was

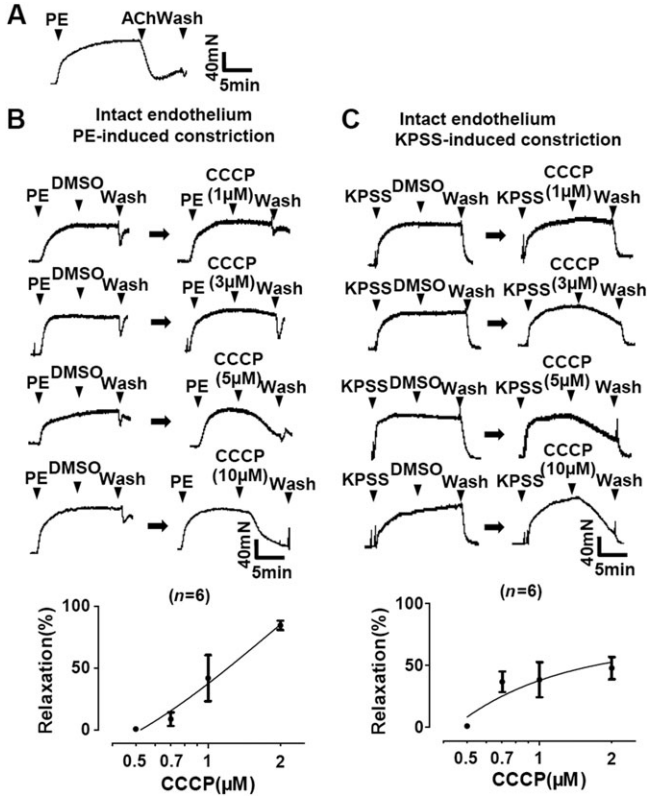

Figure 3

CCCP relaxes PE- and high KPSS-induced constriction of rat thoracic aorta. (A) Original trace demonstrating endothelium-intact rat thoracic aorta. The artery was precontracted with PE (1 μM) and relaxed by ACh (10 μM). (B, C) CCCP induced dose-dependent relaxation in endothelium-intact rat thoracic aorta precontracted with PE (1 μM) and KPSS. The relaxation ratio of CCCP was calculated by subtracting the relaxation ratio of corresponding control (DMSO) to avoid the error induced by natural rundown of the artery tension.

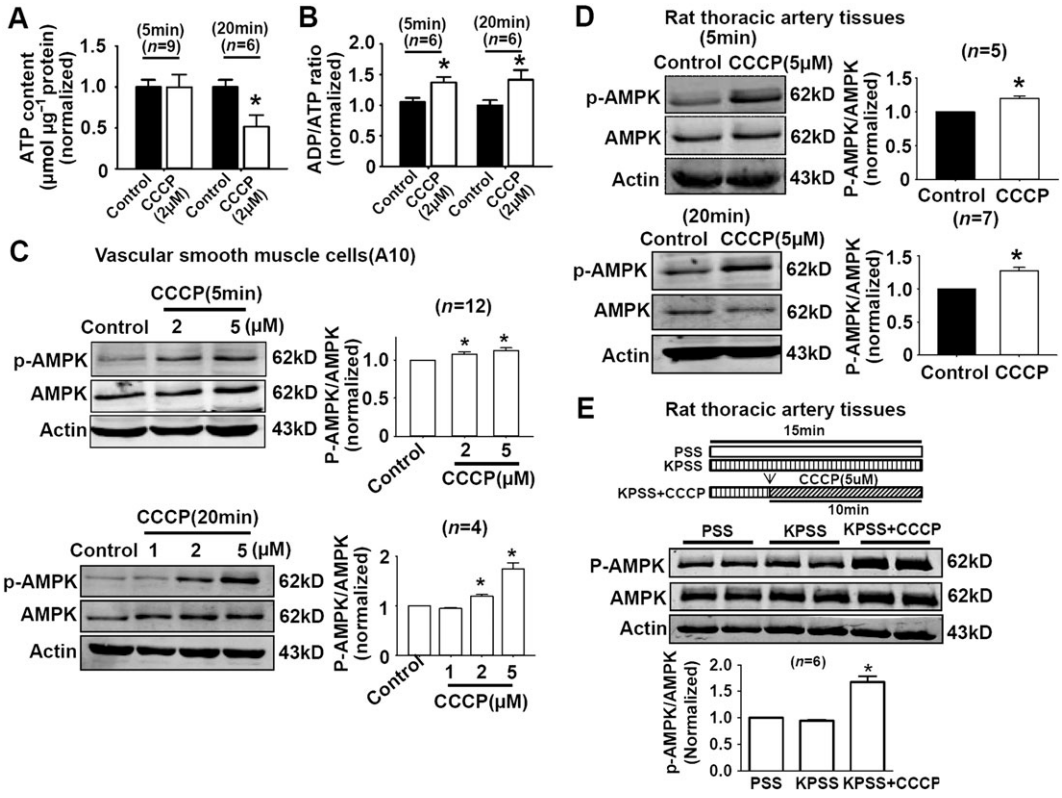

Figure 4

CCCP increases ADP/ATP ratio and activates AMPK. (A) CCCP (2 μM) did not affect the cellular ATP level after 5 min treatment but reduced the cellular ATP level after 20 min treatment in A10 cells. *$P < 0.05$ versus control. (B) CCCP increased the ADP/ATP ratio in A10 cells after 5 and 20 min treatment. *$P < 0.05$ versus control. (C) CCCP activated AMPK after 5 and 20 min treatment in vascular smooth muscle cells (A10). *$P < 0.05$ versus control. The data were normalized to control for avoiding unwanted variations. (D) CCCP activated AMPK in rat thoracic aorta tissues after 5 and 20 min treatment. *$P < 0.05$ versus control. The data were normalized to control for avoiding unwanted variation. (E) CCCP activated AMPK in the presence of KPSS in rat aorta tissues. *$P < 0.05$ versus control (PSS).

potentiated and ATP production decreased. AMPK is activated in response to an increase in the ADP/ATP ratio. Indeed, AMPK was activated after CCCP treatment for 5 and 20 min in vascular smooth muscle cells (A10) (Figure 4C). We further showed that CCCP could activate AMPK in rat aorta tissues after 5 and 20 min treatment (Figure 4D), and CCCP still significantly activated AMPK in the presence of KPSS in rat aorta tissues (Figure 4E).

AMPK activation induces vasodilatation (Goirand *et al.*, 2007; Schneider *et al.*, 2015). Since CCCP activated AMPK in vascular smooth muscle cells and artery tissues, we speculated that the AMPK activation was involved in CCCP-induced vasorelaxation. Compound C is an AMPK inhibitor. Firstly, we tried to use compound C to inhibit AMPK. However, compound C relaxed the constricted artery itself. As shown in Figure S5A, compound C dose-dependently relaxed the rat mesenteric arteries pre-contracted by PE. When the concentration of compound C was reduced to 2 μM, at which it showed no vasorelaxant effects, it also showed no effect on CCCP-induced vasorelaxation (Figure S5B). Therefore, we further used AMPK α1 knockout (−/−) mice rather than compound C to identify the involvement of AMPK in CCCP-induced vasorelaxation. We had shown that CCCP-induced vasorelaxation was endothelium independent, so we used endothelium-intact arteries from AMPK α1 knockout (−/−) mice. As shown in Figure 5A, CCCP-induced aorta relaxation was diminished in AMPKα1 knockout (−/−) mice, indicating that AMPK activation might be involved in CCCP-induced vasorelaxation. We also measured the endothelium-dependent vasorelaxation of arteries from AMPK α1 knockout (−/−) mice and found no difference in the ACh-induced vasorelaxation responses in AMPKα1 knockout (−/−) and wild-type mice (Figure S6). In a previous study it was demonstrated that activation of AMPK α1 but not AMPK α2 induced aortic relaxation in mice in an endothelium- and eNOS-independent manner (Goirand *et al.*, 2007), which was in line with our results.

It has been reported that AMPK activation dilated resistance arteries via activation of sarco-endoplasmic reticulum Ca^{2+} ATPase (SERCA) and BKCa (large-conductance, calcium-activated potassium channel) ($K_{Ca}1.1$)channels in smooth muscle (Schneider *et al.*, 2015). We speculated that the SERCA and BKCa pathways might be involved in CCCP-induced vasorelaxation. We used CPA and tharpsigargin, the two SERCA inhibitors, to examine the role of SERCA in CCCP-induced vasorelaxation. As shown in Figure 5B and C, both CPA and tharpsigargin treatments partially attenuated CCCP-induced vasorelaxation in endothelium-denuded rat mesenteric arteries, indicating that SERCA activation plays a role in CCCP-induced vasorelaxation. Moreover, we

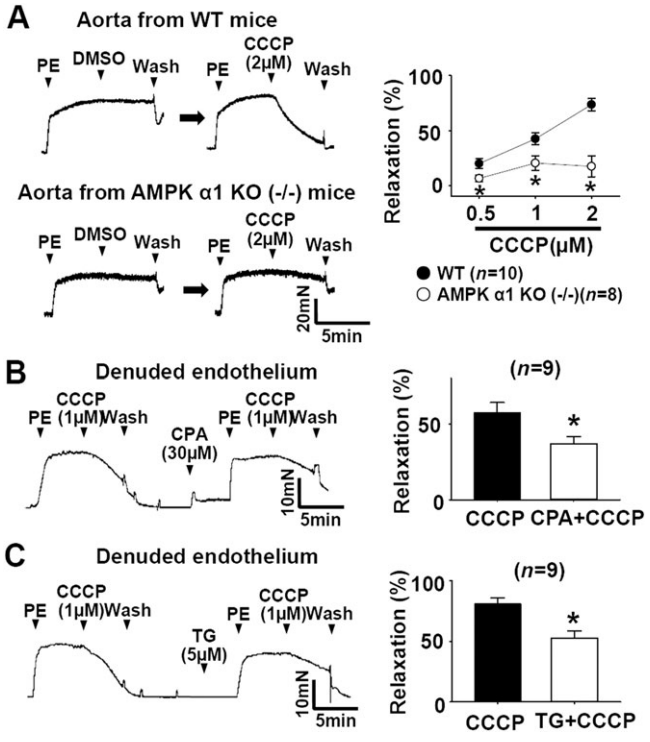

Figure 5

Role of AMPK/SERCA activation in CCCP -induced vasorelaxation. (A) CCCP-induced aorta relaxation was abolished in AMPKα1 knockout (−/−) mice. *$P < 0.05$ versus WT. (B) SERCA inhibitor CPA partially attenuated CCCP-induced vasorelaxation in endothelium-denuded rat mensenteric arteries precontracted with PE (5 μM). *$P < 0.05$ versus CCCP. (C) SERCA inhibitor tharpsigargin (TG) partially attenuated CCCP-induced vasorelaxation in endothelium-denuded rat mensenteric arteries precontracted with PE (5 μM). *$P < 0.05$ versus CCCP.

further used the BKCa channel blocker paxilline and found that, regardless of whether it was used before or after CCCP treatment, it had no significant effect on CCCP-induced vasorelaxation in endothelium-denuded rat mensenteric arteries (data not shown). Paxilline at 1 μM has been shown to inhibit vasodilatation in arterioles (Joerk *et al.*, 2014), but we observed no effect on CCCP-induced vasorelaxation even with 5 μM, indicating that the BKCa channel is not involved in the CCCP-induced vasorelaxation.

CCCP induces vasorelaxation without involving K_{ATP} channel activation in smooth muscle cells

The cytosolic ATP level influences the activity of K_{ATP} channels. Since CCCP as a mitochondrial uncoupler increased the ADP/ATP ratio and decreased ATP production, CCCP-induced vasorelaxation was speculated to be due to the K_{ATP} channel activation. However, in both endothelium-intact and endothelium-denuded rat mesenteric arteries, the K_{ATP} channel blocker glibenclamide and the mitochondrial-specific K_{ATP} channel blocker 5-HD did not affect CCCP-induced vasorelaxation (Figure 6A–6D). We further confirmed that the efficacy of glibenclamide was reliable in our experimental conditions because it inhibited the vasorelaxation induced by K_{ATP} channel activator diazoxide (Figure 6E). Incidentally, the mitochondrial specific K_{ATP} channel blocker 5-HD (100 and 500 μM) was not observed to inhibit diazoxide -induced vasorelaxation, so only the summarized data of 5-HD (100 μM) are shown (Figure 6F). Similarly to the present results, 5-HD was also reported not to block the protection by the K_{ATP} channel agonist diazoxide in heart ischaemia–reperfusion injury (Nadtochiy *et al.*, 2009). Our results indicate that K_{ATP} channels were not involved in the CCCP-induced vasorelaxation.

CCCP increases cytosolic $[Ca^{2+}]_i$, mitoROS production and depolarizes mitochondrial membrane potential in vascular smooth muscle cells (A10)

Because CCCP induced vasorelaxation, we further examined the effects of CCCP on cytosolic $[Ca^{2+}]_i$ in vascular smooth muscle cells (A10). It was very interesting that CCCP treatment increased cytosolic $[Ca^{2+}]_i$ (Figures S7A and S7B), consistent with the report that CCCP treatment increased cytosolic $[Ca^{2+}]_i$ in prostatic cells (Vaur *et al.*, 2000). Ca^{2+}/calmodulin-dependent protein kinase is involved in AMPK activation (Shen *et al.*, 2007; Bair *et al.*, 2009), we further studied the role of the CCCP-induced increase in cytosolic $[Ca^{2+}]_i$ in CCCP-induced AMPK activation in A10 cells by chelating intracellular Ca^{2+} with BAPTA-AM. Ca^{2+} chelation with BAPTA-AM (10 μM) has been shown to inhibit Ca^{2+}-dependent cellular signals (Pfisterer *et al.*, 2011), but it had no effect on CCCP-induced AMPK activation (data not shown), indicating that the increased cytosolic $[Ca^{2+}]_i$ did not contribute to CCCP-induced AMPK activation.

The reports about the effects of CCCP on cellular ROS production are not consistent. CCCP treatment increased ROS production in RKO human colon carcinoma cell lines (Izeradjene *et al.*, 2005) but suppressed high glucose-induced ROS production in human mesangial cells (Kiritoshi *et al.*, 2003) and superoxide generation in mesenteric artery rings from DOCA-salt rats (Viel *et al.*, 2008). We measured the effects of CCCP on mitoROS production in vascular smooth muscle cells (A10) by using mitoSOX staining and found that CCCP treatment slightly increased mitoROS production (Figure 7A and B). We further used mitoTEMPO to scavenge the increased mitoROS to investigate whether the increased ROS was involved in CCCP-induced AMPK activation. MitoTEMPO at concentrations ranging from 25 nM to 200 μM has been used previously in different cell experiments (Dikalova *et al.*, 2010; Tanaka *et al.*, 2012; Reed *et al.*, 2014; Lee *et al.*, 2015; Patel *et al.*, 2015). We found that mitoTEMPO at 5 and 100 μM did not influence the activation of AMPK by CCCP (data not shown), indicating that CCCP-induced ROS increase did not contribute to CCCP-induced AMPK activation in A10 cells.

Finally, we utilized a lipophilic cationic dye TMRM to examine the effects of CCCP on mitochondrial membrane potential in vascular smooth muscle cells (A10). CCCP treatment depolarized mitochondrial membrane potential (Figure 7 C and D), confirming its mitochondrial uncoupling effects.

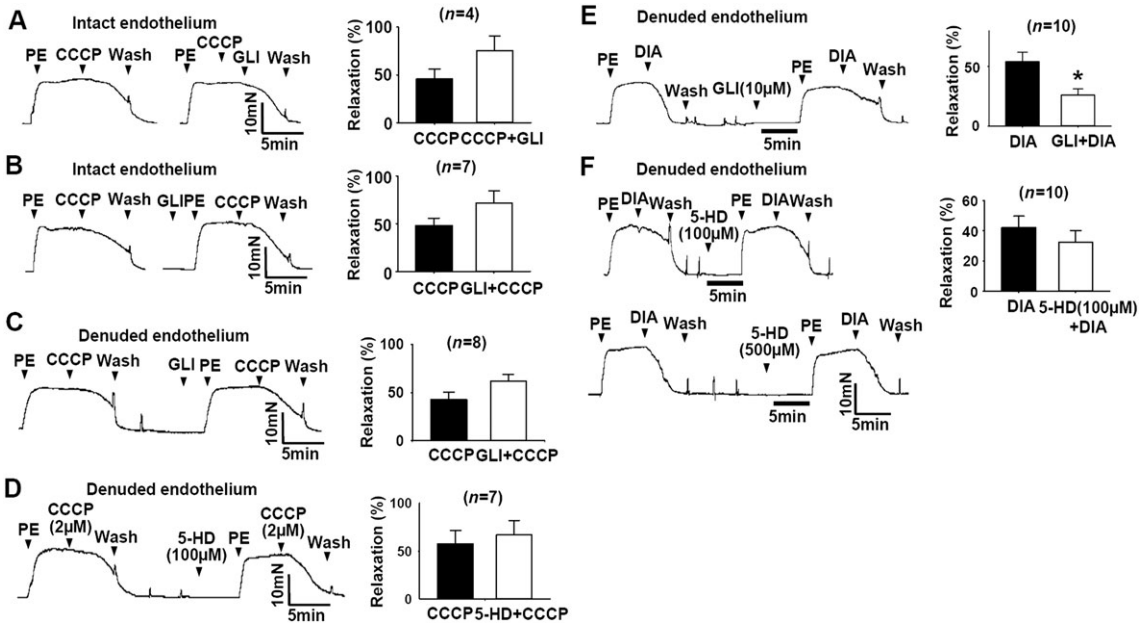

Figure 6

K_{ATP} channel blocker glibenclamide (GLI) and 5-HD do not affect CCCP-induced vasorelaxation. (A, B) The use of glibenclamide before or after CCCP treatment did not affect CCCP-induced vasorelaxation in endothelium-intact rat mesenteric arteries precontracted with PE (5 μM). (C, D) Pretreatment with glibenclamide and 5-HD did not affect CCCP-induced vasorelaxation in endothelium-denuded rat mesenteric arteries precontracted with PE (5 μM). (E) GLI inhibited the vasorelaxation induced by K_{ATP} channel activator diazoxide (DIA) in endothelium-denuded rat mesenteric arteries precontracted with PE (5 μM). *$P < 0.05$ versus DIA (100 μM). (F) The mitochondrial specific K_{ATP} channel blocker 5-HD did not inhibit diazoxide-induced vasorelaxation. The representative recordings with 100 and 500 μM 5-HD are shown in the left panel and the data analysed for 100 μM 5-HD are shown in the right panel.

As mentioned in the Introduction, mild mitochondrial uncoupling is proposed as a protective therapeutic strategy for many disorders. At present, the mild mitochondrial uncoupling is generally induced by using techniques that evoke the overexpression of UCPs. However, the criteria that discriminate mild from complete mitochondrial uncoupling are unclear. Tao *et al*. 2014reported that niclosamide ethanolamine improved glycaemic control and delayed disease progression in db/db mice by inducing mild mitochondrial uncoupling (Tao *et al*. 2014). Niclosamide ethanolamine also reduced ATP production and increased the ADP/ATP ratio in cultured HepG2 cells (Tao *et al*. 2014). We were not sure if CCCP-induced mitochondrial uncoupling in smooth muscle cells was mild or complete in the present conditions, so we measured the cytotoxicity of CCCP in vascular smooth muscle cells (A10). In the functional experiments, 2 μM CCCP was used for up to 20 min (Figure 4). In the cytotoxic studies, we treated A10 cells with 2 μM CCCP for 24 h. CCCP (2 μM) had no significant effect on cell viability after 24 h treatment (Figures S8A and S8B), indicating that CCCP-induced vasorelaxation was not due to the non-specific cytotoxicity of CCCP.

FCCP has similar effects on artery constriction as CCCP

FCCP, an analogue of CCCP, is also widely used to induce mitochondrial uncoupling. We investigated whether FCCP had similar vasoactivity as that of CCCP. As shown in Figure 8A and C, FCCP induced relaxation in both endothelium-intact and endothelium-denuded rat mesenteric arteries precontracted with PE. FCCP pretreatment prevented PE-induced constriction of rat mesenteric arteries with intact or denuded endothelium (Figure 8B and D). These results demonstrate that both FCCP and CCCP had similar vasoactivity.

Discussion

The acute effects of CCCP, a typical mitochondrial uncoupler, on vasoactivity and the potential mechanisms have never been elucidated. In the present study, we demonstrated that CCCP induced vasorelaxation without involving K_{ATP} channel activation in smooth muscle cells of arteries. Our results indicated that the mechanisms of CCCP-induced vasorelaxation were complicated. Although we examined different factors related to vasorelaxation, including AMPK, SERCA, cytosolic $[Ca^{2+}]_i$ and K_{ATP} channels, the CCCP-induced vasorelaxation could not be explained via a unique mechanism. Based on the current understanding and our present results, the schematic of CCCP-induced vasorelaxation is summarized in Figure 9, which showed that CCCP activated different factors contributing to vasorelaxation and vasoconstriction, but the net result was vasorelaxation.

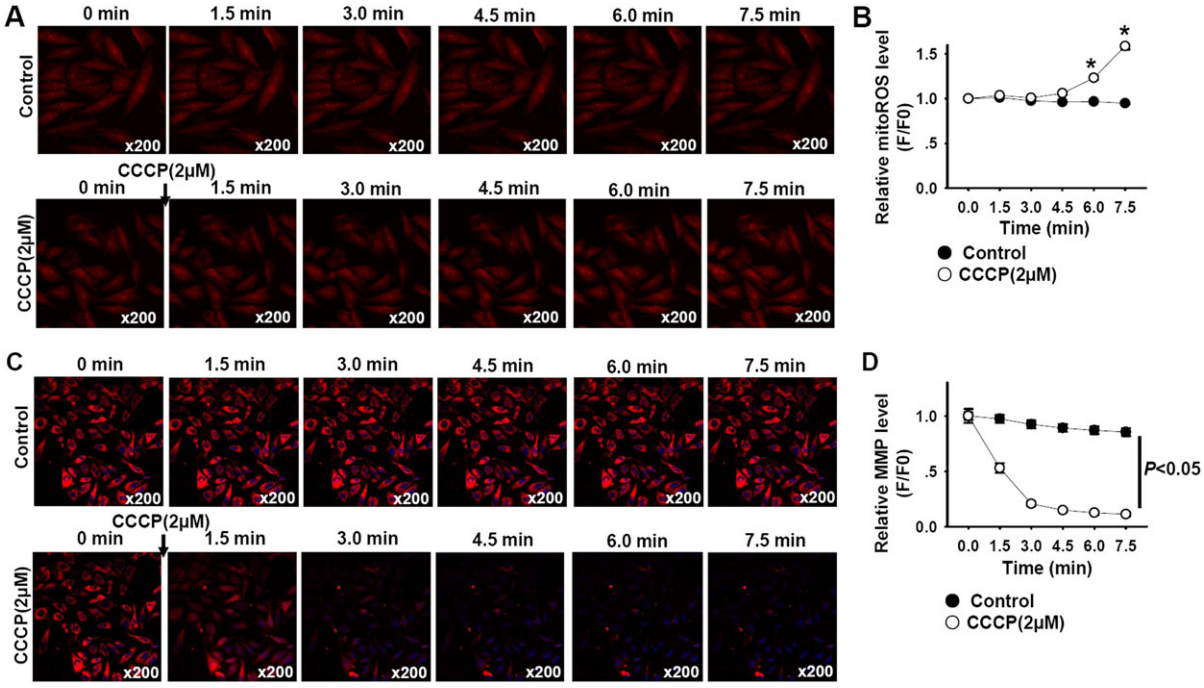

Figure 7

CCCP increases mitoROS production and depolarizes mitochondrial membrane potential in vascular smooth muscle cells (A10). (A) The representative time-lapse images show that CCCP treatment increased mitoROS production. (B) The summarized data of CCCP-induced increase in mitochondrial ROS production. The experiment was carried out in cultured vascular smooth muscle cells (A10). Sixty-eight cells in control group and 68 cells in CCCP (2 μM) group were counted and analysed. *$P < 0.05$ versus control. (C) The representative time-lapse images show that CCCP decreased TMRM fluorescence. (D) The summarized data of CCCP-induced decrease in TMRM intensity. The experiment was carried out in cultured vascular smooth muscle cells (A10). One-hundred and sixty cells in control group and 82 cells in CCCP (2 μM) group were counted and analysed. MMP, mitochondrial membrane potential.

CCCP-induced vasorelaxation and AMPK

AMPK activation is reported to induce vasodilatation in many arterial vessels (Goirand *et al.*, 2007; Schneider *et al.*, 2015). AMPK-induced vasodilatation includes endothelium-dependent and -independent mechanisms. The endothelium-dependent mechanism was considered to be through AMPK-induced eNOS activation (Dolinsky *et al.*, 2010; Zheng *et al.*, 2011). We found that CCCP-induced vasodilatation in rat mesenteric arteries and thoracic aorta was endothelium-independent, and CCCP treatment had no significant effect on eNOS activation in HUVECs, indicating that CCCP-induced vasodilatation was through a direct action of CCCP on vascular smooth muscle cells. The effects of AMPK on vasoactivity have been studied by using AMPK knockout mice. Goirand *et al.* (2007) showed that activation of AMPK α1 but not AMPK α2 was able to induce aortic relaxation in mice, in an endothelium- and eNOS-independent manner (Goirand *et al.*, 2007). Wang *et al.* further showed that AMPK decreased vascular smooth muscle cell contractility by inhibiting p190-GTP-activating protein-dependent Ras homolog gene family member A activation in mesenteric artery and aortas (Wang *et al.*, 2011). A recent work elucidated the endothelium-independent mechanisms of AMPK-induced vasodilatation in detail (Schneider *et al.*, 2015). They showed that AMPK dilated resistance arteries from hamster and mouse via activation of SERCA and BKCa channels in smooth muscle, but BKCa played only a minor role.

Since CCCP activated AMPK in vascular smooth muscle cells and artery tissues, we speculated that AMPK activation was involved in CCCP-induced vasorelaxation. However, the AMPK inhibitor compound C failed to be a suitable pharmacological tool for proving the role of AMPK activation in CCCP-induced vasorelaxation because it relaxed the constricted artery itself. So, we further used an AMPK α1 knockout (−/−) mice model. Although the CCCP-induced aorta relaxation was attenuated in AMPK α1 knockout (−/−) mice, as CCCP is thought to have numerous other effects, such as inhibiting ATP production, depolarizing mitochondrial membrane potential and increasing cytosolic $[Ca^{2+}]_i$, AMPK activation might be involved in CCCP-induced vasorelaxation but is only one of the various mechanisms. SERCA is regarded as the downstream signal of AMPK in AMPK-induced vasorelaxation (Schneider *et al.*, 2015). Our results showed that SERCA inhibitors cyclopiazonic acid and tharpsigargin only partially attenuated CCCP-induced vasorelaxation, further indicating that AMPK/SERCA pathway was not the unique mechanism involved in this effect of CCCP. CCCP is not a pure AMPK activator; it also uncouples mitochondria and reduces ATP production. The mitochondrial uncoupler dinitrophenol was reported to totally abolish the phosphorylation of myosin light chain (MLC) in rat tail artery (Swärd *et al.*, 2002), indicating that inhibition of MLC phosphorylation might also be involved in CCCP's effects.

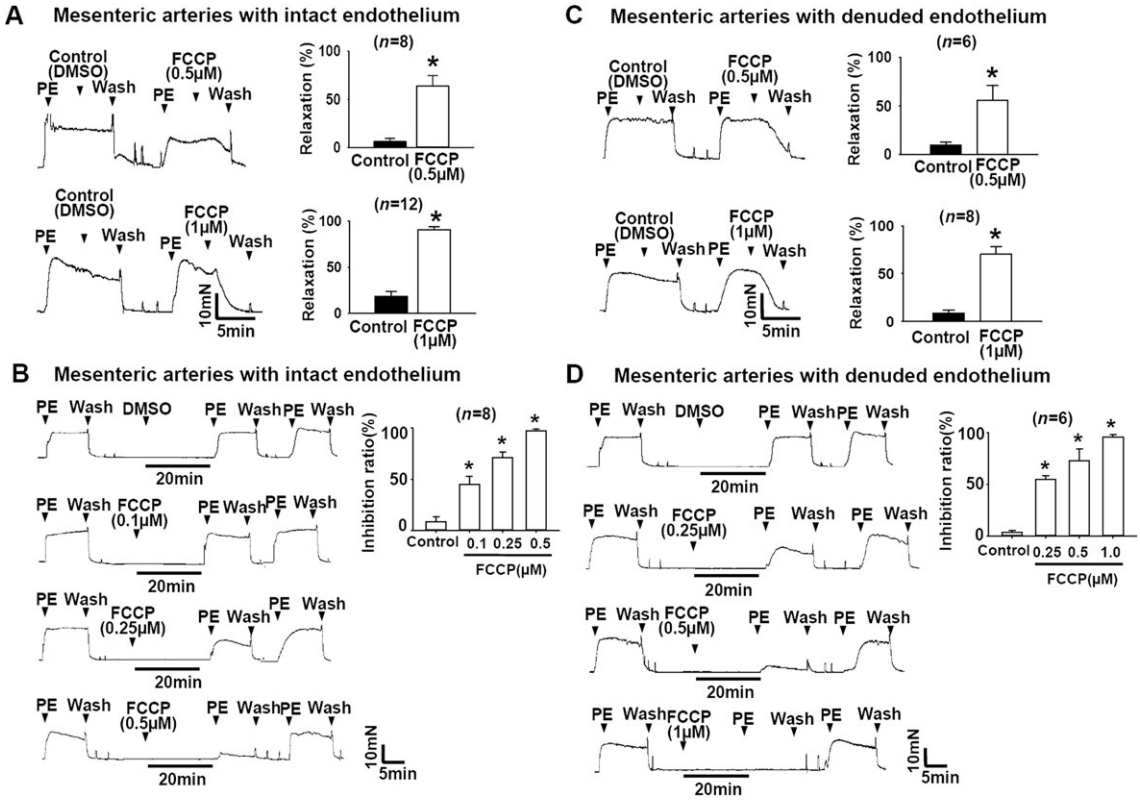

Figure 8

FCCP antagonizes vasoconstriction of rat mesenteric arteries. (A) FCCP induced vasorelaxation in endothelium-intact rat mesenteric arteries pre-contracted with PE (5 μM). $^{**}P < 0.01$ versus control. (B) FCCP pretreatment prevented PE (5 μM)-induced constriction of rat mesenteric arteries with intact endothelium. $^{**}P < 0.01$ versus control. (C) FCCP induced vasorelaxation in endothelium-denuded rat mesenteric arteries pre-contracted with PE (5 μM). $^{**}P < 0.01$ versus control. (D) FCCP pretreatment prevented PE (5 μM)-induced constriction of rat mesenteric arteries with denuded endothelium. $^{*}P < 0.05$ versus control.

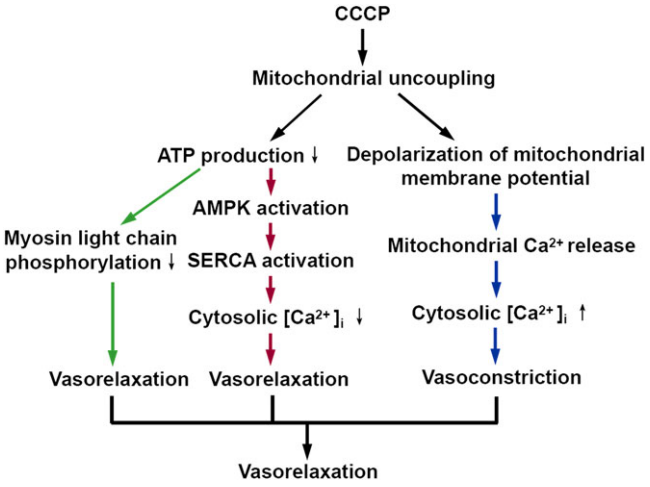

Figure 9

Schematic illustration of the potential mechanism of CCCP-induced vasorelaxation. CCCP activated different factors contributing to vasorelaxation and vasoconstriction, but the net result was vasorelaxation. The schematic was summarized based on the current understanding and our present results.

Although both activation (Schneider *et al.*, 2015) and inhibition (Wyatt *et al.*, 2007; Ross *et al.*, 2011) of BKCa channels by activated AMPK have been reported, we found that BKCa channels contributed less to CCCP-induced vasorelaxation than other mechanisms.

CCCP-induced vasorelaxation and cytosolic $[Ca^{2+}]_i$

We found that, although CCCP induced significant vasodilatation, to a certain extent, it also increased cytosolic $[Ca^{2+}]_i$ in vascular smooth muscle cells. This finding that CCCP increased $[Ca^{2+}]_i$ in A10 cells but relaxed the constricted vessels is an interesting phenomenon. On the one hand, CCCP permeabilizes the mitochondrial inner membrane thereby allowing Ca^{2+} that is normally sequestered and stored within mitochondria to be released into the cytosol; on the other hand, despite the increase in cellular $[Ca^{2+}]_i$, which tends to induce contraction, CCCP-induced inhibition of mitochondrial function still results in vasorelaxation.

SERCA-mediated re-uptake of Ca^{2+} into the sarcoplasmic reticulum SR is an important mechanism of vasorelaxation (Van Hove *et al.*, 2009). Our results showed that SERCA

activation was partially involved in CCCP-induced vasorelaxation; however, the cytosolic $[Ca^{2+}]_i$ was consistently increased after CCCP treatment in smooth muscle cells (A10). We speculated that the increased cytosolic $[Ca^{2+}]_i$ tended to constrict the vessel, whereas the other vasorelaxant actions of CCCP (decreased ATP generation; loss of mitochondrial energy) counteracted the vasoconstriction (Figure 9); therefore, the CCCP-induced vasoactivity and cytosolic $[Ca^{2+}]_i$ changes seemed not to be parallel. Inhibition of oxidative metabolism is often found to decrease the contractility of vascular smooth muscle but not to reduce global $[Ca^{2+}]_i$. In the rat tail artery, mitochondrial inhibitors (rotenone, antimycin A and cyanide) reduced α_1-adrenoceptor-stimulated force but did not reduce global $[Ca^{2+}]_i$ (Swärd *et al.*, 2002).

CCCP-induced vasorelaxation and K_{ATP} channels

CCCP, as well as FCCP, has long been used as a mitochondrial uncoupler to inhibit metabolism, thus activating K_{ATP} channels. In cat ventricular myocytes, CCCP elicited K_{ATP} currents (de Lorenzi *et al.*, 1995) and in rat ventricular myocytes, FCCP activated K_{ATP} channels (Krause *et al.*, 1995). In Xenopus oocytes injected with SUR1, which increases the expression of either $K_{ir}6.2$ or $K_{ir}6.1$ channels, K_{ATP} currents increased when cytosolic ATP levels were lowered by the metabolic inhibitor FCCP (Gribble *et al.*, 1997). However, other works suggested that activation of K_{ATP} channels was not inevitable for the actions of FCCP or CCCP. For instance, in the isolated rat heart, mitochondrial uncoupling with FCCP significantly improved post-ischaemic functional recovery; this cardioprotection was mediated via a ROS-dependent pathway but not by the depletion of cellular ATP or K_{ATP} channel activation (Brennan *et al.*, 2006). Nitroalkenes protected cardiomyocytes against simulated ischaemia–reperfusion injury by inducing mild mitochondrial uncoupling, which was not affected by K_{ATP} channel blockers 5-HD or glibenclamide (Nadtochiy *et al.*, 2009). In the present study, although CCCP increased ADP/ATP ratio and activated AMPK in vascular smooth muscle cells (A10), the K_{ATP} channel blocker glibenclamide and the mitochondrial specific K_{ATP} channel blocker 5-HD did not affect CCCP-induced vasorelaxation, indicating that K_{ATP} channels were not involved in CCCP-induced vasorelaxation. These data answer the question as to whether K_{ATP} channel activation contributes to mitochondrial uncoupler-induced vasorelaxation.

CCCP-induced vasorelaxation and mitoROS

UCPs-induced mitochondrial uncoupling reduces mitoROS generation in different cell types. In endothelial cells, UCP2 overexpression suppressed ROS production in human aortic endothelial cells (Lee *et al.*, 2005); UCP2 silencing led to elevated mitoROS formation in endothelial cells (Koziel *et al.*, 2015) and renal mesangial cells (Di Castro *et al.*, 2013). However, the effects of the mitochondrial uncoupler CCCP on mitoROS production were reported are not consistent. On the one hand, some studies reported that the mitochondrial uncoupler CCCP increased mitoROS production, for instance, in primary mouse sensory neurons (Summers *et al.*, 2014), and human colon carcinoma cell lines (Izeradjene *et al.*, 2005). On the other hand, CCCP was reported to inhibit ROS increase in endothelial cells induced by leptin and homocysteine (Yamagishi *et al.*, 2001; Sethi *et al.*, 2006) and in vascular smooth muscle cells induced by ET-1 (Touyz *et al.*, 2004). A compromised viewpoint considered that nanomolar concentrations of CCCP elevated ROS but micromolar concentrations of CCCP reduced ROS in artery smooth muscle cells (Xi *et al.*, 2005). Our results showed that CCCP at 2 μM gradually increased mitoROS generation in vascular smooth muscle cells.

Conclusions

Our results showed that CCCP treatment significantly activated AMPK in vascular smooth muscle cells and CCCP, as well as FCCP, had a strong vasorelaxant effect on resistant arteries. Activating AMPK not only acts as a therapeutic strategy for metabolic diseases including diabetes and obesity but also for hypertension (Ruderman *et al.*, 2013; Almabrouk *et al.*, 2014). Recently, the chemical mitochondrial uncouplers including 2,4 dinitrophenol (DNP), niclosamide ethanolamine and C4R1 have been shown to be significantly beneficial in hypertriglyceridaemia, insulin resistance and obesity in animal models (Perry *et al.*, 2013; Tao *et al.*, 2014; Kalinovich and Shabalina, 2015; Perry *et al.*, 2015), suggesting that mitochondrial uncouplers could be a distinct class of drugs with therapeutic effects for both metabolic disorders and hypertension, especially for the 'triple H' (hypertension, hyperlipidaemia and hyperglycaemia) patients, if these drugs are shown to have an appropriate pharmacological uncoupling action and no toxicity *in vivo*. Of course, the toxic effects of mitochondrial uncouplers could be overcome by optimizing the drug delivery, similar to the approaches used for DNP; controlled-release oral formulation of DNP and methylated DNP (Perry *et al.*, 2013, 2015). From the results of our study, it is proposed that mitochondrial uncouplers might be a novel type of vasodilator and have potential as anti-hypertensive drugs.

Acknowledgements

We are grateful to Prof. Hong-Liang Li (Collaborative Innovation Center of Model Animal Wuhan University) for gifting the AMPKα1 knockout (-/-) mice.

This work was supported by the National Basic Research Program of China (Grant no. 2012CB517803) and the National Natural Science Foundation of China (Grant nos 81373406, 81421063).

Author contributions

Y-Q.Z., M-Y.L. and J.Y. measured the isometric tension of mesenteric artery. S-L.L, C-L.Z. and X.S. measured the isometric tension of thoracic aorta. J.J. and J-L.G. cultured the cells. M-Y.L., J.J., J-L.G.,Y.T., L-S.Z. and Y-L.B. measured the cytosolic $[Ca^{2+}]_i$, mitoROS and mitochondrial membrane potential of smooth muscle cells. X-L.X., N.H.and X-Z.Z. carried out the western blot experiments. D-L.D designed the project and wrote the paper.

Conflict of interest

The authors declare no conflicts of interest.

Declaration of transparency and scientific rigour

This Declaration acknowledges that this paper adheres to the principles for transparent reporting and scientific rigour of preclinical research recommended by funding agencies, publishers and other organisations engaged with supporting research.

References

Adebiyi A, McNally EM, Jaggar JH (2011). Vasodilation induced by oxygen/glucose deprivation is attenuated in cerebral arteries of SUR2 null mice. Am J Physiol Heart Circ Physiol 301: H1360–H1368.

Alexander SP, Catterall WA, Kelly E, Marrion N, Peters JA, Benson HE *et al.* (2015a). The Concise Guide to PHARMACOLOGY 2015/16: Voltage-gated ion channels. Br J Pharmacol 172: 5904–5941.

Alexander SPH, Fabbro D, Kelly E, Marrion N, Peters JA, Benson HE *et al.* (2015b). The Concise Guide to PHARMACOLOGY 2015/16: Enzymes. Br J Pharmacol 172: 6024–6109.

Alexander SPH, Kelly E, Marrion N, Peters JA, Benson HE, Faccenda E *et al.* (2015c). The Concise Guide to PHARMACOLOGY 2015/16: Transporters. Br J Pharmacol 172: 6110–6202.

Almabrouk TA, Ewart MA, Salt IP, Kennedy S (2014). Perivascular fat, AMP-activated protein kinase and vascular diseases. Br J Pharmacol 171: 595–617.

Bair AM, Thippegowda PB, Freichel M, Cheng N, Ye RD, Vogel SM *et al.* (2009). Ca2+ entry via TRPC channels is necessary for thrombin-induced NF-kappaB activation in endothelial cells through AMP-activated protein kinase and protein kinase Cdelta. J Biol Chem 284: 563–574.

Brennan JP, Southworth R, Medina RA, Davidson SM, Duchen MR, Shattock MJ (2006). Mitochondrial uncoupling, with low concentration FCCP, induces ROS-dependent cardioprotection independent of KATP channel activation. Cardiovasc Res 72: 313–321.

Busiello RA, Savarese S, Lombardi A (2015). Mitochondrial uncoupling proteins and energy metabolism. Front Physiol 6: 36.

Chen C, Hu JT, Tu YJ, Wu JC, Liang J, Gao LL *et al.* (2010). Effects of isosorbide mononitrate on the restoration of injured artery in mice in vivo. Eur J Pharmacol 640: 150–156.

Curtis MJ, Bond RA, Spina D, Ahluwalia A, Alexander SP, Giembycz MA *et al.* (2015). Experimental design and analysis and their reporting: new guidance for publication in BJP. Br J Pharmacol 172: 3461–3471.

de Lorenzi FG, Bridal TR, Spinelli W (1995). Voltage-dependent inhibition of the ATP-sensitive K+ current by the class Ia agent disopyramide in cat ventricular myocytes. J Pharmacol Exp Ther 272: 714–723.

Di Castro S, Scarpino S, Marchitti S, Bianchi F, Stanzione R, Cotugno M *et al.* (2013). Differential modulation of uncoupling protein 2 in kidneys of stroke-prone spontaneously hypertensive rats under high-salt/low-potassium diet. Hypertension 61: 534–541.

Diano S, Horvath TL (2012). Mitochondrial uncoupling protein 2 (UCP2) in glucose and lipid metabolism. Trends Mol Med 18: 52–58.

Dikalova AE, Bikineyeva AT, Budzyn K, Nazarewicz RR, McCann L, Lewis W*et al.* (2010). Therapeutic targeting of mitochondrial superoxide in hypertension. Circ Res 107: 106–116.

Dolinsky VW, Morton JS, Oka T, Robillard-Frayne I, Bagdan M, Lopaschuk GD *et al.* (2010). Calorie restriction prevents hypertension and cardiac hypertrophy in the spontaneously hypertensive rat. Hypertension 56: 412–421.

Eskiocak B, Ali A, White MA (2014). The estrogen-related receptor alpha inverse agonist XCT 790 is a nanomolar mitochondrial uncoupler. Biochemistry 53: 4839–4846.

Figarola JL, Singhal J, Tompkins JD, Rogers GW, Warden C, Horne D *et al.* (2015). SR4 uncouples mitochondrial oxidative phosphorylation, modulates AMP-dependent kinase (AMPK)-mammalian target of rapamycin (mTOR) signaling, and inhibits proliferation of HepG2 hepatocarcinoma cells. J Biol Chem 290: 30321–30341.

Goirand F, Solar M, Athea Y, Viollet B, Mateo P, Fortin D *et al.* (2007). Activation of AMP kinase alpha1 subunit induces aortic vasorelaxation in mice. J Physiol 581: 1163–1171.

Gribble FM, Ashfield R, Ammala C, Ashcroft FM (1997). Properties of cloned ATP-sensitive K+ currents expressed in Xenopus oocytes. J Physiol 498 (Pt 1): 87–98.

Haeusler G, Richards JG, Thorens S (1981). Noradrenaline contractions in rabbit mesenteric arteries skinned with saponin. J Physiol 321: 537–556.

Izeradjene K, Douglas L, Tillman DM, Delaney AB, Houghton JA (2005). Reactive oxygen species regulate caspase activation in tumor necrosis factor-related apoptosis-inducing ligand-resistant human colon carcinoma cell lines. Cancer Res 65: 7436–7445.

Joerk A, Seidel RA, Walter SG, Wiegand A, Kahnes M, Klopfleisch M *et al.* (2014). Impact of heme and heme degradation products on vascular diameter in mouse visual cortex. J Am Heart Assoc 3: ppi: e001220.

Kalinovich AV, Shabalina IG (2015). Novel mitochondrial cationic uncoupler C4R1 is an effective treatment for combating obesity in mice. Biochemistry (Mosc) 80: 620–628.

Kilkenny C, Browne W, Cuthill IC, Emerson M, Altman DG (2010). Animal research: Reporting *in vivo* experiments: the ARRIVE guidelines. Br J Pharmacol 160: 1577–1579.

Kiritoshi S, Nishikawa T, Sonoda K, Kukidome D, Senokuchi T, Matsuo T*et al.* (2003). Reactive oxygen species from mitochondria induce cyclooxygenase-2 gene expression in human mesangial cells: potential role in diabetic nephropathy. Diabetes 52: 2570–2577.

Koziel A, Sobieraj I, Jarmuszkiewicz W (2015). Increased activity of mitochondrial uncoupling protein 2 improves stress resistance in cultured endothelial cells exposed in vitro to high glucose levels. Am J Physiol Heart Circ Physiol 309: H147–H156.

Krause E, Englert H, Gogelein H (1995). Adenosine triphosphate-dependent K currents activated by metabolic inhibition in rat ventricular myocytes differ from those elicited by the channel opener rilmakalim. Pflugers Arch 429: 625–635.

Lee KU, Lee IK, Han J, Song DK, Kim YM, Song HS *et al.* (2005). Effects of recombinant adenovirus-mediated uncoupling protein 2 overexpression on endothelial function and apoptosis. Circ Res 96: 1200–1207.

Lee Y, Kubli DA, Hanna RA, Cortez MQ, Lee HY, Miyamoto S *et al.* (2015). Cellular redox status determines sensitivity to BNIP3-mediated cell death in cardiac myocytes. Am J Physiol Cell Physiol 308: C983–C992.

Ma S, Ma L, Yang D, Luo Z, Hao X, Liu D *et al.* (2010). Uncoupling protein 2 ablation exacerbates high-salt intake-induced vascular dysfunction. Am J Hypertens 23: 822–828.

McGrath JC, Lilley E (2015). Implementing guidelines on reporting research using animals (ARRIVE etc.): new requirements for publication in BJP. Br J Pharmacol 172: 3189–3193.

Nadtochiy SM, Baker PR, Freeman BA, Brookes PS (2009). Mitochondrial nitroalkene formation and mild uncoupling in ischaemic preconditioning: implications for cardioprotection. Cardiovasc Res 82: 333–340.

Park JY, Park KG, Kim HJ, Kang HG, Ahn JD, Kim HS *et al.* (2005). The effects of the overexpression of recombinant uncoupling protein 2 on proliferation, migration and plasminogen activator inhibitor 1 expression in human vascular smooth muscle cells. Diabetologia 48: 1022–1028.

Patel AS, Song JW, Chu SG, Mizumura K, Osorio JC, Shi Y*et al.* (2015). Epithelial cell mitochondrial dysfunction and PINK1 are induced by transforming growth factor-beta1 in pulmonary fibrosis. PLoS One 10: e0121246.

Perry RJ, Kim T, Zhang XM, Lee HY, Pesta D, Popov VB *et al.* (2013). Reversal of hypertriglyceridemia, fatty liver disease, and insulin resistance by a liver-targeted mitochondrial uncoupler. Cell Metab 18: 740–748.

Perry RJ, Zhang D, Zhang XM, Boyer JL, Shulman GI (2015). Controlled-release mitochondrial protonophore reverses diabetes and steatohepatitis in rats. Science 347: 1253–1256.

Pfisterer SG, Mauthe M, Codogno P, Proikas-Cezanne T (2011). Ca2+/calmodulin-dependent kinase (CaMK) signaling via CaMKI and AMP-activated protein kinase contributes to the regulation of WIPI-1 at the onset of autophagy. Mol Pharmacol 80: 1066–1075.

Reed KN, Wilson G, Pearsall A, Grishko VI (2014). The role of mitochondrial reactive oxygen species in cartilage matrix destruction. Mol Cell Biochem 397: 195–201.

Ross FA, Rafferty JN, Dallas ML, Ogunbayo O, Ikematsu N, McClafferty H *et al.* (2011). Selective expression in carotid body type I cells of a single splice variant of the large conductance calcium- and voltage-activated potassium channel confers regulation by AMP-activated protein kinase. J Biol Chem 286: 11929–11936.

Ruderman NB, Carling D, Prentki M, Cacicedo JM (2013). AMPK, insulin resistance, and the metabolic syndrome. J Clin Invest 123: 2764–2772.

Schneider H, Schubert KM, Blodow S, Kreutz CP, Erdogmus S, Wiedenmann M *et al.* (2015). AMPK dilates resistance arteries via activation of SERCA and BKCa channels in smooth muscle. Hypertension 66: 108–116.

Sethi AS, Lees DM, Douthwaite JA, Dawnay AB, Corder R (2006). Homocysteine-induced endothelin-1 release is dependent on hyperglycaemia and reactive oxygen species production in bovine aortic endothelial cells. J Vasc Res 43: 175–183.

Shen QW, Zhu MJ, Tong J, Ren J, Du M (2007). Ca2+/calmodulin-dependent protein kinase kinase is involved in AMP-activated protein kinase activation by alpha-lipoic acid in C2C12 myotubes. Am J Physiol Cell Physiol 293: C1395–C1403.

Soltoff SP (2004). Evidence that tyrphostins AG10 and AG18 are mitochondrial uncouplers that alter phosphorylation-dependent cell signaling. J Biol Chem 279: 10910–10918.

Southan C, Sharman JL, Benson HE, Faccenda E, Pawson AJ, Alexander SP *et al.* (2016). The IUPHAR/BPS Guide to PHARMACOLOGY in 2016: towards curated quantitative interactions between 1300 protein targets and 6000 ligands. Nucl. Acids Res. 44: D1054–D1068.

Summers DW, DiAntonio A, Milbrandt J (2014). Mitochondrial dysfunction induces Sarm1-dependent cell death in sensory neurons. J Neurosci 34: 9338–9350.

Sun B, Huo R, Sheng Y, Li Y, Xie X, Chen C *et al.* (2013). Bone morphogenetic protein-4 mediates cardiac hypertrophy, apoptosis, and fibrosis in experimentally pathological cardiac hypertrophy. Hypertension 61: 352–360.

Swärd K, Dreja K, Lindqvist A, Persson E, Hellstrand P (2002). Influence of mitochondrial inhibition on global and local [Ca(2+)](i) in rat tail artery. Circ Res 90: 792–799.

Tanaka A, Jin Y, Lee SJ, Zhang M, Kim HP, Stolz DB *et al.* (2012). Hyperoxia-induced LC3B interacts with the Fas apoptotic pathway in epithelial cell death. Am J Respir Cell Mol Biol 46: 507–514.

Tao H, Zhang Y, Zeng X, Shulman GI, Jin S (2014). Niclosamide ethanolamine-induced mild mitochondrial uncoupling improves diabetic symptoms in mice. Nat Med 20: 1263–1269.

Tian XY, Wong WT, Xu A, Lu Y, Zhang Y, Wang L *et al.* (2012). Uncoupling protein-2 protects endothelial function in diet-induced obese mice. Circ Res 110: 1211–1216.

Touyz RM, Yao G, Viel E, Amiri F, Schiffrin EL (2004). Angiotensin II and endothelin-1 regulate MAP kinases through different redox-dependent mechanisms in human vascular smooth muscle cells. J Hypertens 22: 1141–1149.

Van Hove CE, Van der Donckt C, Herman AG, Bult H, Fransen P (2009). Vasodilator efficacy of nitric oxide depends on mechanisms of intracellular calcium mobilization in mouse aortic smooth muscle cells. Br J Pharmacol 158: 920–930.

Vaur S, Sartor P, Dufy-Barbe L (2000). Calcium store depletion induced by mitochondrial uncoupling in prostatic cells. Gen Physiol Biophys 19: 265–278.

Viel EC, Benkirane K, Javeshghani D, Touyz RM, Schiffrin EL (2008). Xanthine oxidase and mitochondria contribute to vascular superoxide anion generation in DOCA-salt hypertensive rats. Am J Physiol Heart Circ Physiol 295: H281–H288.

Wang S, Liang B, Viollet B, Zou MH (2011). Inhibition of the AMP-activated protein kinase-alpha2 accentuates agonist-induced vascular smooth muscle contraction and high blood pressure in mice. Hypertension 57: 1010–1017.

Wang YC, Hu CW, Liu MY, Jiang HC, Huo R, Dong DL (2013). Copper induces vasorelaxation and antagonizes noradrenaline-induced vasoconstriction in rat mesenteric artery. Cell Physiol Biochem 32: 1247–1254.

Wyatt CN, Mustard KJ, Pearson SA, Dallas ML, Atkinson L, Kumar P *et al.* (2007). AMP-activated protein kinase mediates carotid body excitation by hypoxia. J Biol Chem 282: 8092–8098.

Xi Q, Cheranov SY, Jaggar JH (2005). Mitochondria-derived reactive oxygen species dilate cerebral arteries by activating Ca2+ sparks. Circ Res 97: 354–362.

Xie X, Zhao Y, Ma CY, Xu XM, Zhang YQ, Wang CG *et al.* (2015). Dimethyl fumarate induces necroptosis in colon cancer cells through

GSH depletion/ROS increase/MAPKs activation pathway. Br J Pharmacol 172: 3929–3943.

Yamagishi SI, Edelstein D, Du XL, Kaneda Y, Guzman M, Brownlee M (2001). Leptin induces mitochondrial superoxide production and monocyte chemoattractant protein-1 expression in aortic endothelial cells by increasing fatty acid oxidation via protein kinase A. J Biol Chem 276: 25096–25100.

Zheng Q, Yuan Y, Yi W, Lau WB, Wang Y, Wang X *et al*. (2011). C1q/TNF-related proteins, a family of novel adipokines, induce vascular relaxation through the adiponectin receptor-1/AMPK/eNOS/nitric oxide signaling pathway. Arterioscler Thromb Vasc Biol 31: 2616–2623.

Supporting Information

Additional Supporting Information may be found in the online version of this article at the publisher's web-site:

http://dx.doi.org/10.1111/bph.13578

Figure S1 (A) The endothelium denudation of rat mesenteric artery was confirmed by absence of Ach (1 μM)-induced relaxation. (B,C) Original traces showing that CCCP induced dose-dependent relaxation in endothelium-denuded rat mesenteric arteries pre-contracted with PE (5 μM) and the summarized data. The relaxation ratio of CCCP was calculated by subtracting the relaxation ratio of corresponding control (DMSO) to avoid the error induced by natural rundown of the artery tension. (D,E) Original traces showing that CCCP induced dose-dependent relaxation in endothelium-denuded rat mesenteric arteries pre-contracted with KPSS and the summarized data. The relaxation ratio of CCCP was calculated by subtracting the relaxation ratio of corresponding control (DMSO) to avoid the error induced by natural rundown of the artery tension.

Figure S2 CCCP pretreatment inhibited PE(5 μM)- and KPSS-induced constriction of rat mesenteric arteries with denuded endothelium. The inhibitory effect of CCCP was relieved after washout of CCCP. $^{**}P < 0.01$ vs DMSO (control).PE, phenylephrine.

Figure S3 (A) The endothelium denudation of rat thoracic aorta was confirmed by absence of Ach (1 μM)-induced relaxation. (B,C) CCCP induced dose-dependent relaxation in endothelium-denuded rat thoracic aorta precontracted with PE and KPSS. The relaxation ratio of CCCP was calculated by subtracting the relaxation ratio of corresponding control (DMSO) to avoid the error induced by natural rundown of the artery tension. PE, phenylephrine.

Figure S4 The effects of CCCP on eNOS activity in human umbilical vein endothelial cells (HUVECs). CCCP (1 μM and 10 μM) did not affect the eNOS and p-eNOS expressions in protein level in HUVECs after 5 and 15 min treatment. The data were normalized to control for avoiding unwanted variation.

Figure S5 Compound C has vasorelaxant effects on endothelium-denuded rat mesenteric arteries. (A) Compound C dose-dependently relaxed the rat mesenteric arteries precontracted by PE (5 μM). (B) Compound C at 2 μM concentration showed no vasorelaxant effect, but it also showed no effect on CCCP-induced vasorelaxation. PE, phenylephrine.

Figure S6 No difference of Ach-induced vasorelaxation in aorta from AMPK α1 knockout (−/−) and wild type mice. WT, wild type(n = 10); KO, AMPK α1 KO (−/−)(n = 8). PE (1 μM), Ach (10 μM).

Figure S7 CCCP increases cytosolic [Ca2+]i in vascular smooth muscle cells(A10). (A) The representative time-lapse images showed that CCCP treatment increased cytosolic $[Ca^{2+}]^{i}$. (B) The summarized data of CCCP-induced increase of cytosolic $[Ca^{2+}]^{i}$. The experiment was carried out in cultured vascular smooth muscle cells (A10). Eighty one cells in control group and seventy seven cells in CCCP(2 μM) group were counted and analysed.

Figure S8 The cytotoxicity of CCCP in vascular smooth muscle cells (A10). (A)CCCP (2 μM) had no significant effect on A10 cell viability after 24 h treatment. The cell viability was measured by using MTT method. (n = 7). (B) The LIVE/DEAD® Viability/Cytotoxicity assay showed that CCCP (2 μM) did not induce cell death after 24 h treatment. Total 2656 cells in control group and total 1900 cells in CCCP group from three independent experiments were analysed. The live cells fluoresce green and dead cells fluoresce red in this assay. The data were normalized to the mean of control for avoiding unwanted variation.